

Time-Resolved Spin-Torque Switching and Enhanced Damping in Permalloy/Cu/Permalloy Spin-Valve Nanopillars

N. C. Emley, I. N. Krivorotov, O. Ozatay, A. G. F. Garcia, J. C. Sankey, D. C. Ralph, and R. A. Buhrman

Cornell University, Ithaca, New York 14853-2501, USA

(Received 1 November 2005; published 19 June 2006)

We report time-resolved measurements of current-induced reversal of a free magnetic layer in Permalloy/Cu/Permalloy elliptical nanopillars at temperatures $T = 4.2$ K to 160 K. Comparison of the data to Landau-Lifshitz-Gilbert macrospin simulations of the free layer switching yields numerical values for the spin torque and the Gilbert damping parameters as functions of T . The damping is strongly T dependent, which we attribute to the presence of an antiferromagnetic oxide layer around the perimeter of the Permalloy free layer. This adventitious antiferromagnetic oxide can have a major impact on spin-torque phenomena.

DOI: 10.1103/PhysRevLett.96.247204

PACS numbers: 85.75.-d, 75.75.+a, 81.65.Mq

Experiments [1–4] have shown that a spin-polarized current passed through a nanomagnet can excite a dynamic response as the result of a spin torque (ST) applied by the conduction electrons [5,6]. The potential for technological impact of this ST effect has inspired research in dc-current-induced microwave oscillations [3,7] and hysteretic switching [1,2,4] in current perpendicular to the plane (CPP) nanopillars and nanoconstrictions. Typically, ST switching data are obtained through the use of slow current ramp rates (~ 1 mA/s), but fast pulses ($\sim 10^{10}$ mA/s) access the regime where thermal activation of the moment over a current-dependent barrier [8,9] does not play a major role in the switching process. This ST-driven regime [10] is advantageous for the quantitative examination of the ST parameters due to the computational accessibility of numerically integrating the phenomenological Landau-Lifshitz-Gilbert (LLG) equation for short durations.

Here we report time-resolved measurements of the ST-driven switching event in Cu 100/Py 20/Cu 6/Py 2/Cu 2/Pt 30 (in nm, Py = Ni₈₁Fe₁₉) CPP spin-valve nanopillar structures at both temperatures $T = 4.2$ K to 160 K. We compare our experimental results with LLG simulations in the macrospin approximation and find good agreement between simulation and measurement. At higher T we find that the strength of the ST exerted per unit current is in reasonable numerical accord with recent model calculations, and that the phenomenological damping parameter α_0 for the nanomagnet excitations is both anomalously high, as suggested by previous pulsed current measurements [11], and T dependent. The strong T variation of α_0 , in conjunction with an irregular variation of the nanomagnet switching fields $H_{S,i}$ at low T , points to the presence of an adventitious antiferromagnetic (AF) oxide layer around the perimeter of the ferromagnetic (F) free layer that has a major effect on the nanomagnet dynamics driven by a ST.

The nanopillar devices employed in this study were fabricated using a process described elsewhere [12]. A slow ramp rate ST scan is shown in Fig. 1(a) for sample 1, a 60×190 nm² ellipse. In Fig. 1(b) we show parallel (P)

to antiparallel (AP) switching events for sample 1, averaged over 10 000 switches, taken at pulsed current amplitudes $I = 1.07$ mA and 2.13 mA at $T = 40$ K. The measured signal is a time-resolved voltage drop $|\Delta R|$ from the giant magnetoresistance (GMR) of the sample as the free layer switches from P to AP orientation, where $\Delta R \equiv R_x(\text{AP}) - R_x(\text{P})$ and R_x is the 4-point device resistance. The data have been normalized to $M_x = +1(-1) \{R_x(\text{P}) [R_x(\text{AP})]\}$ for simple comparison with simulated switching events, described below. The abrupt (~ 200 ps) jump from $M_x = -1$ to 1 at time = 0 is not a switching event but is simply the rising edge of the current pulse. The more gradual transition between P ($M_x = 1$) and AP (return to $M_x = -1$) is the envelope coming from averaging over thousands of individual switching events, each following a trajectory determined by initial conditions randomized by stochastic thermal fluctuations of the free layer. We define the switching time t_{switch} as the time elapsed be-

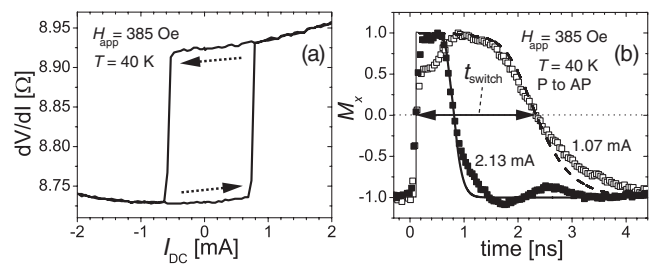


FIG. 1. (a) Slow ramp rate ST switching as measured by the GMR effect for sample 1 at $T = 40$ K and $H_{\text{app}} = 385$ Oe, which opposes the average dipole field so that $H_{\text{app}} + H_{\text{dip}} \approx 0$. (b) Pulsed current P to AP switching measured for the same sample at $I = 1.07$ mA (\square) and 2.13 mA (\blacksquare). AP to P switching data (not shown) are similar in both time and I scales. The data (symbols) have been normalized to $M_x = \pm 1$ for simple comparison with the simulation (lines). The measured $\Delta R(40 \text{ K}) = 0.195 \Omega$. Pulse shape distortions are due to the setup [see Ref. [13]].

tween 50% of the signal rise and 50% of the signal drop as indicated in Fig. 1(b) [13].

To obtain a quantitative understanding of the ST switching, we simulate the nanomagnet dynamics by numerical integration of the LLG equation in the macrospin approximation with an added Slonczewski-type ST term.

$$\begin{aligned} \frac{d\hat{m}}{dt} = & \gamma \left\{ \hat{m} \times [\vec{H}_{\text{eff}} + \vec{H}_{\text{Lang}}(T')] \right. \\ & - \alpha(\theta) \hat{m} \times (\hat{m} \times [\vec{H}_{\text{eff}} + \vec{H}_{\text{Lang}}(T')]) \\ & \left. - \frac{I\hbar g(\theta)}{eM_s(T)(\text{area} \cdot d) \sin\theta} \hat{m} \times \hat{p} \times \hat{m} \right\}. \quad (1) \end{aligned}$$

Here γ is the gyromagnetic ratio, \hat{m} is the unit vector of the free layer macrospin, \hat{p} is the spin polarization axis, θ is the in-plane angle between them, $g(\theta)$ is the ST function, $M_s(T)$ is the free layer magnetization, as measured separately for a continuous 2 nm Py film in a Cu/Py/Cu trilayer that was exposed to the same heat treatments as the nanopillars, where $M_s(4.2 \text{ K}) = 650 \text{ emu/cm}^3$, $d (= 2 \text{ nm})$ is the nanomagnet thickness, $\text{area} = \frac{\pi}{4} ab$ is its lateral area with dimensions a and b that are estimated by OOMMF simulations [14] (see below), and \vec{H}_{eff} is the sum of external \vec{H}_{ext} , in-plane \vec{H}_{K} , and out-of-plane \vec{H}_{\perp} anisotropy fields. For the simulations \vec{H}_{K} was as measured at 4.2 K and then scaled by $M_s(T)/M_s(4.2 \text{ K})$ for different T , while \vec{H}_{\perp} was assumed to be $4\pi M_s(T)$ as appropriate for a very thin nanomagnet. \vec{H}_{ext} is the sum of the magnetostatic dipole field from the fixed layer \vec{H}_{dip} and the in-plane applied field \vec{H}_{app} from the electromagnet, which is adjusted to compensate for the average value of \vec{H}_{dip} so $\vec{H}_{\text{ext}} \approx \vec{0}$.

The initial conditions of the simulation are set by $\theta_i = \theta_0 + \theta_{\text{rand}}(T)$, with $\theta_0 = 0^\circ$ (P to AP) or 180° (AP to P). The random angle $\theta_{\text{rand}}(T)$ is treated as a Gaussian with a standard deviation $\sqrt{k_B T / 2E_0(T)}$, where $E_0(T) = E_0(4.2 \text{ K}) [M_s(T)/M_s(4.2 \text{ K})]^2$ is the uniaxial anisotropy energy. $E_0(4.2 \text{ K})$, a , and b are estimated from $T = 0$, 2D OOMMF simulations of Py elliptical disks having H_{K} and ΔR values similar to those measured at 4.2 K. The lateral area ($\frac{\pi}{4} ab$) is estimated to 12% uncertainty with this method. Ohmic heating effects during the current pulse are taken into account by raising the device temperature to $T' = \sqrt{T^2 + 10.23 \text{ (K/mV)}^2 [R_x(T)I]^2}$ [9]. A Langevin field $\vec{H}_{\text{Lang}}(T')$ accounts for thermal fluctuations during the dynamic trajectory, fluctuating randomly in three dimensions with a standard deviation $\sqrt{2\alpha_0 k_B T' \mu_0 / \gamma M_s(T') (\text{area} \cdot d) \Delta t}$, where $\Delta t = 1 \text{ ps}$ is the time step [8,10,15]. Gilbert damping is assigned an angular dependence $\alpha(\theta) = \alpha_0 [1 - \nu \sin^2\theta / (1 - \nu^2 \cos^2\theta)]$, where $\nu = 0.33$ for Py/Cu/Py nanopillars [16], but the addition of this angle dependence had only a small effect on the simulation results.

The ST function is approximated by $g(\theta) = A \sin\theta / (1 + B \cos\theta)$, where A and B are phenomenological parameters [11,17,18]. We use α_0 , A , and B as

T -dependent fitting parameters to match simulated with measured values of $1/t_{\text{switch}}$ versus I for each T , where we allow α_0 to be different for the two switching directions. In Fig. 1(b) we plot the average of 2000 simulated P to AP switching events at $T = 40 \text{ K}$ alongside the normalized data for sample 1 with the best fit simulation yielding $A = 0.5$, $B = 0.11$, and $\alpha_0 = 0.048$. Since the current step in the simulation turns on instantaneously, an average $\frac{1}{2}$ -rise time of 112 ps, measured from data as in Fig. 1(b), has been added to all simulated t_{switch} . We plot measured $1/t_{\text{switch}}$ versus I for AP to P and P to AP switching at $T = 160 \text{ K}$, 40 K, and 4.2 K for sample 2, an $80 \times 180 \text{ nm}^2$ ellipse, together with best fit simulations, all of which are averages over 2000 events, in Fig. 2(a) and 2(b), respectively. Simulations out to long switching times ($1/t_{\text{switch}} < 0.1 \text{ ns}^{-1}$) allow for good estimates of the $1/t_{\text{switch}} \rightarrow 0$ intercepts $I_{c0}^{\pm}(T)$, which are the critical currents ($+ = \text{P to AP}$) defining the onset of ST-driven switching. These should depend on the ST and damping parameters as $I_{c0}^{\pm}(T) \propto \alpha_0 M_s^2(T)$ [10]. A striking result from these measurements is the strong T dependence of $I_{c0}^{\pm}(T)/M_s^2(T)$ [Fig. 2(a) inset], which varies by more than 60% over the entire T range, where the upturns at low T indicate a strong T dependence of the ST, damping, or both.

In Fig. 3 the best fit values for α_0 , A , and B are plotted as functions of T for sample 2. Uncertainties in the fit parameters, $\Delta\alpha_0 = 0.0035$, $\Delta A = 0.025$, and $\Delta B = 0.045$, are found through an exploration of parameter space about the best fit values. Accounting for these T dependencies, the theoretical prediction of $I_{c0}^{\pm}(T) \propto \alpha_0^{\pm}(T) M_s^2(T) \times [1 \pm B(T)]/A(T)$ agrees with the measurement to within 10% over the entire range of T . All four devices that were extensively studied show an amplitude and T dependence of α_0 very similar to that of Fig. 3(a); a gradual but significant increase with decreasing T below 160 K, above which the devices are thermally unstable, followed by a stronger increase starting below 60 K–40 K. For $T < 60 \text{ K}$ the trends in the T dependence of the ST parameters A and B vary from sample to sample, but for $T > 60 \text{ K}$ both consistently show a very mild dependence on T as illustrated in Fig. 3(b). For the four samples studied in detail, A at 40 K ranged from 0.5 to 0.68 and B varied from 0.11 to

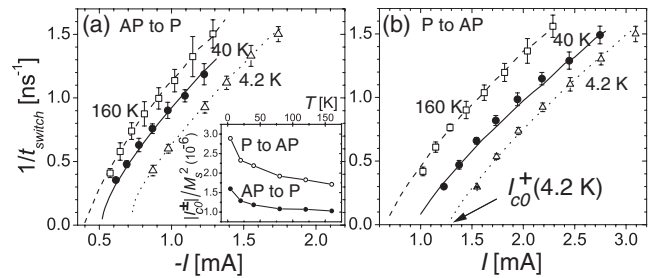


FIG. 2. Measured (symbols) and simulated (lines) $1/t_{\text{switch}}$ vs I for sample 2 at $T = 160 \text{ K}$ (\square), 40 K (\bullet), and 4.2 K (\triangle) for (a) AP to P and (b) P to AP switching. Simulations to $1/t_{\text{switch}} \approx 0$ yield estimates of the intercepts $I_{c0}^{\pm}(T)$. (a) Inset: $I_{c0}^{\pm}(T)/M_s^2(T)$.

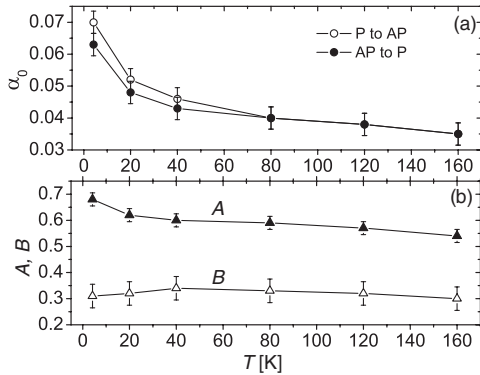


FIG. 3. Best fit parameters (a) damping α_0 [for P to AP (\circ) and AP to P (\bullet) switching] and (b) ST parameters A (\blacktriangle) and B (\triangle) as functions of T from matching simulated with measured values of $1/t_{\text{switch}}$ vs I for each T for sample 2.

0.35. In general, A decreased by 10% or 20% in going from 40 K to 160 K while B varied by 10% or less. These values of A and B and the variation with $T > 60$ K can be compared with the results of a two-channel model [19] with which the measured GMR parameters, $R_x(T)$ and $\Delta R(T)$, can be used to predict the ST parameters [20]. This model predicts $A = 0.52$ and $B = 0.36$ at 40 K, with A decreasing to 0.47 at 160 K and B essentially constant, in reasonable accord with the data given the experimental uncertainties in nanomagnet size and alignment.

The value 0.035 obtained for α_0 for sample 2 at 160 K is in accord with 300 K ST switching results obtained with thicker nanomagnets [11] but is much higher than the intrinsic damping in unpatterned Py films [21]. While spin pumping [16] could be playing a role, the strong variation of α_0 at low T where $\Delta R(T)$ is constant suggests it is not the dominant factor. Instead we attribute the significant T dependence of α_0 to the presence of a weak AF layer on the sidewalls of the nanopillar. Although no such AF layer was deliberately deposited, the exposure of the nanopillars to air after ion mill definition undoubtedly oxidized the sidewalls [22], thus allowing for an AF oxide to form and act to enhance the low T damping of the nanomagnets in a manner similar to that observed previously for air-exposed Py films [23,24].

We observe distinct signatures of NiO, an AF, in x-ray photoemission spectroscopy measurements of air-exposed, unpatterned Py films, and evidence for this adventitious AF oxide on the nanopillar sidewalls is given in Fig. 4 where a series of 4.2 K minor loop field scans of sample 3, an 80×180 nm² ellipse, shows that the free layer switching fields H_{S1} and H_{S2} can vary substantially. We interpret this as arising from the stochastic nature of the incomplete reorientation of the AF domains with each nanomagnet reversal at low T . In the blocking temperature regime, partial reorientation, rather than reversal, of the exchange coupled AF domains is generally invoked to explain the magnetic rotational hysteresis found with ensembles of surface oxidized F nanoparticles (i.e., nanomagnets) as well as the

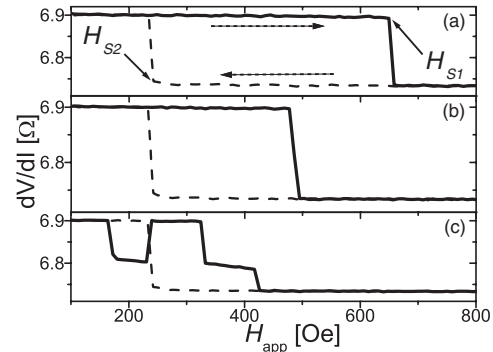


FIG. 4. Selected 4.2 K minor loop GMR scans of sample 3, cooled in $H_{\text{app}} = 0$. While the most commonly observed field-induced reversal of the free layer is shown as in (a) quite often the reversal occurs at lower values of H_{S1} as in (b). Variations in H_{S2} to higher values (not shown) are also observed. Solid lines are for H_{app} increasing. In some instances the magnetic reversal takes place via an intermediate step as in (c). This behavior is attributed to stochastic reorientations of AF domains of the surface oxide on the nanopillar sidewalls (see text).

training effect in extended area AF/F bilayer films, where the exchange bias field is gradually reduced upon multiple F layer reversals and the reversal broadened [25,26]. The average blocking temperature of native oxide AF layers on Py is low and the *net* exchange field weak for extended films [23,24]. However, the local exchange strength between Py and an individual NiO domain can be quite strong below the latter's Néel temperature [25,26]. For an individual nanomagnet it is reasonable to expect that the limited number of Py grains (~ 20 nm diameter), and hence of the associated surface oxide grains, results in the reorientations of the AF domains not always being the same upon multiple reversals. If several AF domains fall into an advantageous set of orientations the effect on the subsequent reversal of the nanomagnet could be quite pronounced due to its small size. Although Py has no significant anisotropy, apart from the nanomagnet shape anisotropy, NiO can induce biaxial anisotropy on Py [27] explaining the 2-step magnetization reversal that we sometimes observe, as illustrated in Fig. 4(c). Such behavior cannot be explained via the micromagnetics of a simple, purely ferromagnetic nanopillar structure.

It is important to note that the slow ramp rate ST switching events at low T for these devices show good reproducibility, with little variation from one sweep to another, as should be the case because ST switching currents are only weakly sensitive to effective field variations. Our simulations show that variations of \tilde{H}_K within the range observed in the field switching measurements would not affect our results by more than the uncertainties given above. The strength of this low T AF exchange biasing varies from device to device, with some samples showing no random variations in $H_{S,i}$. We do not believe that fluctuations of this sort have affected any previously published conclusions from our group. Nevertheless, the seemingly stochas-

tic variations in H_{S1} and H_{S2} and the rarer two-step reversal indicate clearly the presence of an AF layer that should influence the properties of all nanopillar ST devices.

Exchange biasing in AF/Py films has been demonstrated to enhance the dissipation of dynamic magnetic energy. This effect is often attributed to two-magnon scattering arising from local variations in the interfacial exchange coupling [21,28,29]. An alternative mechanism, suggested by Fig. 4, is that the exchange coupling to the nanomagnet induces rapid reorientations of the AF domains during its reversal. Since the AF domains do not all move coherently with the nanomagnet at low T their reorientation will effectively dissipate precessional energy. Even as T is increased and the AF grains become progressively less blocked and follow the precessing nanomagnet more completely, to the extent that the response remains incoherent, this can still result in domain drag or the “slow-relaxer” dissipation process [30]. This could be an important contributor to the greater than intrinsic damping that persists to higher T in ST-driven nanomagnets [11].

Most ST device fabrication processes currently employed expose the sides of the free layer nanomagnet to some level of an oxidizing ambient at some point, either during or after processing and to our knowledge there have been no reports of actively protecting the sidewalls from oxidation. We suggest that the native AF oxide layer that forms can have substantial, previously under-appreciated consequences for the ST behavior, leading to a substantially enhanced damping parameter which directly increases the critical currents for switching. The presence of this AF perimeter layer may also alter the boundary conditions that should be employed in micromagnetic modeling of the free layer nanomagnet behavior and affect the dynamical modes of ST-driven precession. In addition, it is important to note that two-magnon scattering, and also possibly the slow-relaxer process, does not conserve the magnitude of the local precessing moment, as assumed by the LLG equation. While we believe that our analysis in terms of this simple phenomenological model and our finding of enhanced T -dependent damping remain justified, based on the success of the LLG equation in describing previous ST experiments, it would also be of considerable value to analyze the dynamics of ST-excited nanomagnets coupled to thin AF layers using more comprehensive microscopic approaches [31].

In summary, we have performed time-resolved measurements of the ST-driven switching of a Py nanomagnet at $T = 4.2$ K to 160 K that reveal a strong T dependence of I_{c0}^{\pm} at low T . LLG macrospin simulations successfully describe the switching, yielding values of the parameterized ST function $g(\theta) = A \sin\theta/(1 + B \cos\theta)$ and the phenomenological damping parameter. We find α_0 to be high, >0.03 , and strongly T dependent, which we attribute to the pinning behavior of a thin AF oxide layer on the sidewall of the nanomagnet. The values of A and B are in fair numerical agreement with those calculated from the two-channel

model using the measured magnetoresistance values of the nanopillar spin valve. There is, however, considerable device-to-device variation in the ST asymmetry parameter B . The presence of an AF oxide layer can have a major effect on the nanomagnet dynamics. Controlling this layer will be important in optimizing ST-driven behavior.

This research was supported by ARO No. DAAD19-01-1-0541, and by NSF through the NSEC support of the Cornell Center for Nanoscale Systems. Additional support was provided by NSF through use of the facilities of the Cornell Nanoscale Facility NNIN and the facilities of the Cornell MRSEC.

-
- [1] J. A. Katine *et al.*, Phys. Rev. Lett. **84**, 3149 (2000).
 - [2] S. Urzhidn *et al.*, Phys. Rev. Lett. **91**, 146803 (2003).
 - [3] S. I. Kiselev *et al.*, Nature (London) **425**, 380 (2003).
 - [4] J. Grollier *et al.*, Appl. Phys. Lett. **78**, 3663 (2001).
 - [5] J. C. Slonczewski, J. Magn. Magn. Mater. **159**, L1 (1996).
 - [6] L. Berger, Phys. Rev. B **54**, 9353 (1996).
 - [7] W. H. Rippard *et al.*, Phys. Rev. Lett. **95**, 067203 (2005).
 - [8] Z. Li and S. Zhang, Phys. Rev. B **69**, 134416 (2004).
 - [9] I. N. Krivorotov *et al.*, Phys. Rev. Lett. **93**, 166603 (2004).
 - [10] R. H. Koch, J. A. Katine, and J. Z. Sun, Phys. Rev. Lett. **92**, 088302 (2004).
 - [11] P. M. Braganca *et al.*, Appl. Phys. Lett. **87**, 112507 (2005).
 - [12] N. C. Emley *et al.*, Appl. Phys. Lett. **84**, 4257 (2004).
 - [13] Jitter noise in the triggering of the oscilloscope prevents the complete removal of distortions in the pulse shape coming from the pulser and amplifier, giving a slowly oscillating background and a shoulder in the current step. These introduce a maximum error of only 7% in the measurements of t_{switch} and are not significant.
 - [14] M. J. Donahue and D. G. Porter, *OOMMF User's Guide*, Version 1.0 Interagency Report No. 6376, NIST, Gaithersburg, MD (1999).
 - [15] S. E. Russek *et al.*, Phys. Rev. B **71**, 104425 (2005).
 - [16] Y. Tserkovnyak, A. Brataas, and G. E. W. Bauer, Phys. Rev. B **67**, 140404(R) (2003).
 - [17] J. C. Slonczewski, J. Magn. Magn. Mater. **247**, 324 (2002).
 - [18] J. Xiao, A. Zangwill, and M. D. Stiles, Phys. Rev. B **70**, 172405 (2004).
 - [19] T. Valet and A. Fert, Phys. Rev. B **48**, 7099 (1993).
 - [20] A. G. F. Garcia (to be published).
 - [21] M. C. Weber *et al.*, J. Appl. Phys. **97**, 10A701 (2005).
 - [22] Any ferromagnetic material redeposited on the nanopillar sidewalls during ion milling would also be at least partially oxidized during subsequent exposure to air.
 - [23] S. H. Charap and E. Fulcomer, J. Appl. Phys. **42**, 1426 (1971).
 - [24] C. E. Patton and C. H. Wilts, J. Appl. Phys. **38**, 3537 (1967).
 - [25] J. Nogués and I. K. Schuller, J. Magn. Magn. Mater. **192**, 203 (1999).
 - [26] J. Nogués *et al.*, Phys. Rep. **422**, 65 (2005).
 - [27] R. P. Michel *et al.*, Phys. Rev. B **58**, 8566 (1998).
 - [28] R. D. McMichael *et al.*, J. Appl. Phys. **83**, 7037 (1998).
 - [29] S. M. Rezende *et al.*, Phys. Rev. B **63**, 214418 (2001).
 - [30] R. D. McMichael *et al.*, J. Appl. Phys. **87**, 6406 (2000).
 - [31] J. Lindner *et al.*, Phys. Rev. B **68**, 060102(R) (2003).